

An Efficient FDTD Algorithm to Analyze Skewed Periodic Structures Impinged by Obliquely Incident Wave

M. Bai, B. Liang, and H. Ma

School of Electronic and Information Engineering
Beihang University, Beijing, 100191, China
mbai@buaa.edu.cn, girder21@ee.buaa.edu.cn, yoyo@ee.buaa.edu.cn

Abstract — An efficient wideband finite-difference time-domain (FDTD) method is proposed to analyze arbitrarily skewed periodic structures at oblique incidence. The method is free of complex step-by-step phase processing caused by the oblique incident plane wave and the stagger unit cells, and the provided periodic boundary condition (PBC) is as simple to implement as in the normal incidence case. A numerical example is simulated respectively by our method in one-time calculation over a wideband and the previous dual plane wave method requiring multiple repeated runs, which verifies the validity and efficiency of the proposed method.

Index Terms — Finite difference time domain (FDTD), oblique incidence, periodic structures, skewed grids, wideband.

I. INTRODUCTION

In the field of electromagnetism, periodic structures have been drawing great attentions for tens of years, in a wide range of applications in frequency selective surfaces (FSS) [1-3], electromagnetic band gap (EBG) devices [4] and phased antenna arrays [5], etc. To analyze periodic structures, finite-difference time-domain (FDTD) algorithm [6] has been extensively utilized, and in general only one unit cell needs to be modeled and simulated according to the Floquet theory [5]. A lot of work has been done on FDTD algorithm by incorporating periodic boundary conditions (PBC) to deal with periodic structures, at both normal and oblique incidence [7-11]. When the object is illuminated by a normally incident plane wave, the electromagnetic fields on the boundary of one side of the rectangular unit cell are identical to those on the other side, so that a wideband response can be conveniently obtained by stimulating a transient pulse [8]. However, for the oblique incidence case, the time delay in the time domain caused by the phase shift between corresponding boundaries in the frequency domain leads to difficulties in using the PBCs. By proposing the dual plane wave method, [7] tackled the obstacle at oblique incidence,

but only a single frequency is fixed in each calculation. Afterwards, the split-FDTD method [6,8], some implicit-FDTD methods [9-11] and the material independent FDTD method [12] were proposed respectively, successfully realizing the ability of wideband calculation at oblique incidence.

It is worthwhile pointing out that the aforementioned implementations of the PBCs are developed to deal with regular rectangular periodic structures, as shown in Fig. 1 (a). Nonetheless, a number of applications with arbitrarily skewed adjacent rows in periodic structures as shown in Fig. 1 (b) are frequently encountered. For example, in order to obtain superior bandwidth and stability to different incident angles and polarizations, the FSS needs to be designed with a specific skewed angle [1]. Therefore, the analysis of skewed periodic structures is necessary and important. In terms of the FDTD method treating skewed periodic structures, the dual plane wave method to analyze the periodic phased array with skewed grids was adopted in [13], but each calculation is only fixed on one single frequency at the specific incident angle. Reference [14] presented another method to deal with the issue, employing the constant horizontal wavenumber approach. Although in each calculation the frequencies in a wideband are involved, the corresponding incident angle of each frequency is different from each other, because of the horizontal wavenumber being fixed. Therefore, it can be seen that for a specific incident angle, this method still fails to retain the wideband capacity of the FDTD.

In this paper, the field transformation [15] is employed in the FDTD algorithm, to analyze periodic structures with arbitrary skewed grids impinged by the obliquely incident plane wave at specific angles. We prove that the field transformation, which is the basic treatment to realize wideband FDTD analysis at oblique incidence in [8-12], is capable of dealing with the skewed periodic structures as well. The split-FDTD method is extended into the PBCs for skewed grids, and the updating equations are presented. The validity of the method is verified by a numerical example, which provides the results calculated by the dual plane wave

FDTD method as a comparison.

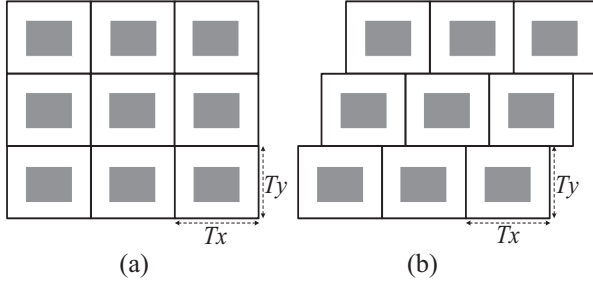


Fig. 1. Periodic structures with: (a) regular rectangular grids, and (b) arbitrarily skewed grids.

II. IMPLEMENTATION OF THE PROPOSED METHOD

Here, three dimensional structures which are periodic in the x - and y -directions with skewed grids in the x -direction are considered. The oblique incident plane wave is launched along the angles θ and φ . Hence, the PBC of any electromagnetic field component Φ is expressed as:

$$\Phi(x+rT_x+s\Delta x, y+sT_y) = \Phi(x, y) \cdot e^{-j[k_x(rT_x+s\Delta x)+k_y sT_y]}, \quad (1)$$

where r and s are any integers, k_x and k_y are the components of wavenumber in the x - and y - directions respectively, which are calculated as:

$$\begin{aligned} k_x &= k \cdot \sin \theta \cdot \cos \varphi, \\ k_y &= k \cdot \sin \theta \cdot \sin \varphi, \end{aligned} \quad (2)$$

where k is the wavenumber of the excited plane wave in free space. It can be seen that the PBC along the y -direction is the same as that of the regular rectangular periodic structures, but it is more complex along the x -direction. In order to use the field transformation to remove the phase shift in the Maxwell's equations, a set of auxiliary variables is introduced as:

$$\begin{aligned} \mathbf{P}(x, y) &= \frac{\mathbf{E}(x, y)}{\eta_0} \cdot e^{j(k_x x + k_y y)}, \\ \mathbf{Q}(x, y) &= \mathbf{H}(x, y) \cdot e^{j(k_x x + k_y y)}, \end{aligned} \quad (3)$$

where η_0 is the impedance of free space. By replacing Φ in (1) with \mathbf{E} and \mathbf{H} respectively and substituting (3) into (1), we obtain:

$$\begin{aligned} \mathbf{P}(x+rT_x+s\Delta x, y+sT_y) &= \mathbf{P}(x, y), \\ \mathbf{Q}(x+rT_x+s\Delta x, y+sT_y) &= \mathbf{Q}(x, y). \end{aligned} \quad (4)$$

Obviously, it has been proved that the PBCs of the transformed fields \mathbf{P} and \mathbf{Q} possess the same forms as the case of normal incidence, without the phase shift. Therefore, it is confirmed that the previous work on wideband FDTD analysis to analyze regular rectangular periodic structures at oblique incidence can be extended to deal with skewed ones. In this paper, we choose to employ the split-FDTD method to develop the

implementation.

Considering a lossless anisotropic medium, by substituting (3) into Maxwell's equations, a set of transformed equations is obtained as:

$$j\omega \frac{\epsilon_{rx}}{c} P_x = \frac{\partial Q_z}{\partial y} - \frac{\partial Q_y}{\partial z} - j\omega \bar{k}_y Q_z + j\omega \bar{k}_z Q_y, \quad (5a)$$

$$j\omega \frac{\epsilon_{ry}}{c} P_y = \frac{\partial Q_x}{\partial z} - \frac{\partial Q_z}{\partial x} - j\omega \bar{k}_z Q_x + j\omega \bar{k}_x Q_z, \quad (5b)$$

$$j\omega \frac{\epsilon_{rz}}{c} P_z = \frac{\partial Q_y}{\partial x} - \frac{\partial Q_x}{\partial y} - j\omega \bar{k}_x Q_y + j\omega \bar{k}_y Q_x, \quad (5c)$$

$$j\omega \frac{\mu_{rx}}{c} Q_x = \frac{\partial P_y}{\partial z} - \frac{\partial P_z}{\partial y} - j\omega \bar{k}_z P_y + j\omega \bar{k}_y P_z, \quad (5d)$$

$$j\omega \frac{\mu_{ry}}{c} Q_y = \frac{\partial P_z}{\partial x} - \frac{\partial P_x}{\partial z} - j\omega \bar{k}_x P_z + j\omega \bar{k}_z P_x, \quad (5e)$$

$$j\omega \frac{\mu_{rz}}{c} Q_z = \frac{\partial P_x}{\partial y} - \frac{\partial P_y}{\partial x} - j\omega \bar{k}_y P_x + j\omega \bar{k}_x P_y, \quad (5f)$$

where

$$\bar{k}_x = \sin \theta \cdot \cos \varphi / c, \quad \bar{k}_y = \sin \theta \cdot \sin \varphi / c, \quad \bar{k}_z = 0, \quad (6)$$

and c is the speed of light. Although \bar{k}_z is zero, it is kept in (5) in order to maintain the symmetry and the cyclic feature of the equations. To conserve space, only (5c) is processed in detail to present the split method in the following. By defining a new variable P_{za} , P_z is split into two parts as:

$$P_z = P_{za} + \frac{c}{\epsilon_{rz}} (\bar{k}_y Q_x - \bar{k}_x Q_y), \quad (7a)$$

where

$$j\omega \frac{\epsilon_{rz}}{c} P_{za} = \frac{\partial Q_y}{\partial x} - \frac{\partial Q_x}{\partial y}. \quad (7b)$$

Similarly, the split form of the other five components can be written conveniently. It can be seen that (7b) is exactly the ordinary formed FDTD formula, so that P_{za} can be obtained in the conventional iteration manner. With regard to the absorbing layers, the auxiliary differential equation (ADE) treatment [16] is utilized to implement the perfect matched layers (PML). By substituting Q_y and Q_x into (7a), and noting that $\bar{k}_z = 0$, P_z can be obtained as:

$$P_z = \left(1 - \frac{c^2 \bar{k}_x^2}{\epsilon_{rz} \mu_{ry}} - \frac{c^2 \bar{k}_y^2}{\epsilon_{rz} \mu_{rx}}\right)^{-1} \left(P_{za} - \frac{c}{\epsilon_{rz}} \bar{k}_x Q_{ya} + \frac{c}{\epsilon_{rz}} \bar{k}_y Q_{xa}\right). \quad (8)$$

It should be noted that since the time step of P_z and P_{za} is n , that of Q_{ya} and Q_{xa} should be n as well, rather than $n-1/2$. Therefore, other than the leapfrog updates of the conventional FDTD, in each half-time-step, all the components need to be updated. Moreover, in order to retain the centered nature of the method, spatial averaging of Q_{ya} and Q_{xa} is also needed. Therefore, the discretization of (8) is written as:

$$P_z \Big|_{i,j,k}^n = \left[1 - \frac{c^2 \bar{k}_x^2}{\varepsilon_{rz} \mu_{ry}} - \frac{c^2 \bar{k}_y^2}{\varepsilon_{rz} \mu_{rx}} \right]^{-1} \cdot \left\{ P_{za} \Big|_{i,j,k}^n - \frac{c}{2\varepsilon_{rz}} \bar{k}_x (Q_{ya} \Big|_{i,j,k}^n + Q_{ya} \Big|_{i-1,j,k}^n) + \frac{c}{2\varepsilon_{rz}} \bar{k}_y (Q_{xa} \Big|_{i,j,k}^n + Q_{xa} \Big|_{i,j-1,k}^n) \right\}. \quad (9)$$

Similarly, Q_z is updated by:

$$Q_z \Big|_{i,j,k}^n = \left[1 - \frac{c^2 \bar{k}_x^2}{\mu_{rz} \varepsilon_{ry}} - \frac{c^2 \bar{k}_y^2}{\mu_{rz} \varepsilon_{rx}} \right]^{-1} \cdot \left\{ Q_{za} \Big|_{i,j,k}^n - \frac{c}{2\varepsilon_{rz}} \bar{k}_y (P_{xa} \Big|_{i,j,k}^n + P_{xa} \Big|_{i+1,j,k}^n) + \frac{c}{2\varepsilon_{rz}} \bar{k}_x (P_{ya} \Big|_{i,j,k}^n + P_{ya} \Big|_{i+1,j,k}^n) \right\}. \quad (10)$$

By substituting (9) and (10) into the counterpart formulas of (7a) respectively, the other four components can be updated as:

$$P_x \Big|_{i,j,k}^n = P_{xa} \Big|_{i,j,k}^n - \frac{c}{2\varepsilon_{rx}} \bar{k}_y (Q_z \Big|_{i,j,k}^n + Q_z \Big|_{i-1,j,k}^n), \quad (11a)$$

$$P_y \Big|_{i,j,k}^n = P_{ya} \Big|_{i,j,k}^n + \frac{c}{2\varepsilon_{ry}} \bar{k}_x (Q_z \Big|_{i,j,k}^n + Q_z \Big|_{i-1,j,k}^n), \quad (11b)$$

$$Q_x \Big|_{i,j,k}^n = Q_{xa} \Big|_{i,j,k}^n + \frac{c}{2\mu_{rx}} \bar{k}_y (P_z \Big|_{i,j,k}^n + P_z \Big|_{i+1,j,k}^n), \quad (11c)$$

$$Q_y \Big|_{i,j,k}^n = Q_{ya} \Big|_{i,j,k}^n - \frac{c}{2\mu_{ry}} \bar{k}_x (P_z \Big|_{i,j,k}^n + P_z \Big|_{i+1,j,k}^n). \quad (11d)$$

Hence, the updating equations have been fully presented. The stability condition of the split method for a square cell and $\bar{k}_x = \bar{k}_y$ is [6]:

$$c\Delta t / \Delta s \leq \cos^2 \theta / \sqrt{2 + \cos^2 \theta}. \quad (12)$$

In terms of other cases, the rigorous stability condition is quite complicated [6], but the maximum allowed values along with θ are not significantly discrepant from (12). Therefore, it can be seen that when the incident angle is close to grazing ($\theta=90^\circ$), implicit methods such as those of [10] and [11] are more practical to be extended to the case of skewed grids.

When updating the aforementioned FDTD formulas, extra care of y -direction boundaries needs to be taken, compared with regular rectangular periodic structures. The schematic diagram of the FDTD grid arrangement for arbitrarily skewed periodic structures is shown in Fig. 2. Each unit cell ($T_x \times T_y$) is meshed using $N_x \times N_y$ grid cells ($dx \times dy$), and $N_x=5$, $N_y=4$ are set here as an example. lx and α are the skewed shift and angle respectively, of which the calculation relationship is:

$$lx = T_y / \tan \alpha. \quad (13)$$

The unit cell A in the center is the simulating object, while others surrounded by red lines are its neighboring unit cells. For any field Ψ on the boundaries in the x -direction, the PBC is the same as the conventional one which can be written as:

$$\begin{aligned} \Psi(i-1, j) &= \Psi(Nx, j) \quad \text{while } i=1, \\ \Psi(i+1, j) &= \Psi(1, j) \quad \text{while } i=Nx. \end{aligned} \quad (14)$$

For Ψ on the y -directional boundaries, two cases need to be discussed respectively:

1) *On the top boundary when $\Psi(i, j+1)$ are needed:*

From (4) we can obtain:

$$\Psi(x, y) = \Psi(x + Tx - lx, y - T_y), \quad (15)$$

and its discretized form when $j=Ny$ can be written as:

$$\Psi(i, j+1) = \Psi(i + Tx - lx, 1). \quad (16)$$

In Fig. 2, the fields $\Psi(i, Ny+1)$ of the unit cell A are denoted by solid green triangles on the top boundary, while the fields $\Psi(i+Tx-lx, 1)$ lying on the corresponding positions on the bottom boundary of A are indicated by the same marks. Since generally the skewed shift is not multiple integer of dx , the hollow green triangles are needed for interpolations. It should be noted that once the index of the hollow mark is larger than Nx , the cyclic shift is necessary to be utilized. Therefore, (16) can be rewritten as:

$$\begin{aligned} \Psi(i, Ny+1) &= \omega_2 \cdot \Psi(i + i_1, 1) + \omega_1 \cdot \Psi(i + i_2, 1) \\ i_1 &= \begin{cases} \left\lceil \frac{Tx - lx}{dx} \right\rceil & (\text{if } \left\lceil \frac{Tx - lx}{dx} \right\rceil \leq Nx) \\ \left\lceil \frac{Tx - lx}{dx} \right\rceil - Nx & (\text{if } \left\lceil \frac{Tx - lx}{dx} \right\rceil > Nx) \end{cases} \\ i_2 &= \begin{cases} i_1 + 1 & (\text{if } i_1 + 1 \leq Nx) \\ i_1 + 1 - Nx & (\text{if } i_1 + 1 > Nx) \end{cases} \\ \omega_1 &= \frac{Tx - lx}{dx} - \left\lceil \frac{Tx - lx}{dx} \right\rceil \\ \omega_2 &= 1 - \omega_1, \end{aligned} \quad (17)$$

where $\lceil \cdot \rceil$ is the truncating function, ω_1 and ω_2 are the normalized distance between the solid mark and the hollow marks on its left and right hands respectively.

2) *On the bottom boundary when $\Psi(i, j-1)$ are needed:* Similar to (16), the boundary condition for $\Psi(i, j-1)$ when $j=1$ is:

$$\Psi(i, j-1) = \Psi(i + lx, Ny). \quad (18)$$

Thus the fields $\Psi(i, 0)$ of the unit cell A are denoted by solid blue circles on the bottom boundary in Fig. 2. Similar to (17), the PBC of $\Psi(i, j-1)$ while $j=1$ can be written as:

$$\Psi(i, 0) = \omega_2 \cdot \Psi(i+i_1, Ny) + \omega_1 \cdot \Psi(i+i_2, Ny)$$

$$i_1 = \begin{cases} \left\lceil \frac{lx}{dx} \right\rceil & (\text{if } \left\lceil \frac{lx}{dx} \right\rceil \leq Nx) \\ \left\lceil \frac{lx}{dx} \right\rceil - Nx & (\text{if } \left\lceil \frac{lx}{dx} \right\rceil > Nx) \end{cases}$$

$$i_2 = \begin{cases} i_1 + 1 & (\text{if } i_1 + 1 \leq Nx) \\ i_1 + 1 - Nx & (\text{if } i_1 + 1 > Nx) \end{cases}$$

$$\omega_1 = \frac{lx}{dx} - \left\lceil \frac{lx}{dx} \right\rceil$$

$$\omega_2 = 1 - \omega_1. \quad (19)$$

Therefore, by utilizing (14), (17) and (19), the fields on the boundaries for updating the FDTD formulas can be resolved. In the particular case when lx and $T_x - lx$ are the integer multiples of dx , (17) and (19) are capable as well, with $\omega_1=0$ and $\omega_2=1$ respectively. It is worthwhile pointing out that the fields locating on the positions $(i \pm 1/2, j \pm 1/2)$ are not necessary to be arranged specifically or marked in Fig. 2, since the criterion of their positions in the interpolation process is thoroughly dependent on the grid cell positions, i.e., (i, j) .

It can be seen that the implementation of the proposed method to deal with general skewed periodic structures at oblique incidence is as simple and straightforward as the normal incident case. Owing to the confirmation of (4), the method is free of careful studies on the phase shift in individual boundary parts, which has to be taken in the dual plane wave method [13] and constant horizontal wavenumber method [14].

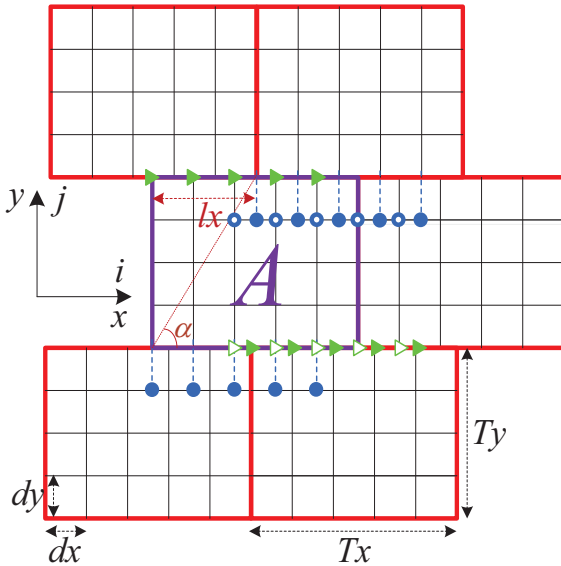


Fig. 2. Schematic diagram of the arbitrarily skewed FDTD grids.

III. NUMERICAL RESULTS

To demonstrate the performance of our method, an example of a Jerusalem Cross FSS (JCFSS) between two anisotropic lossless media ($\epsilon_{rx}=2.2$, $\epsilon_{ry}=1.1$, $\epsilon_{rz}=1.5$) is implemented, as shown in Fig. 3. The unit cell period is $T_x=T_y=6$ mm, the thickness of the JCFSS is 0.625 mm, and the thickness of the substrate is 2 mm. The skewed angle is $\alpha=60^\circ$. The incident plane wave is propagating along the direction $\theta=30^\circ$ and $\varphi=50^\circ$, and both the TM and TE cases are investigated. The structure is firstly simulated by our wideband method, using a sine modulated Gaussian pulse centered at 15 GHz and with 20 GHz bandwidth as the excitation. The grid cell size is $\Delta x=\Delta y=\Delta z=0.125$ mm, and the time step is $\Delta t=\Delta z/(5 \cdot c)$. As a comparison, the example is also simulated by the dual plane wave method, which is repeated 41 times in the frequency range from 5 to 25 GHz by 0.5 GHz frequency step.

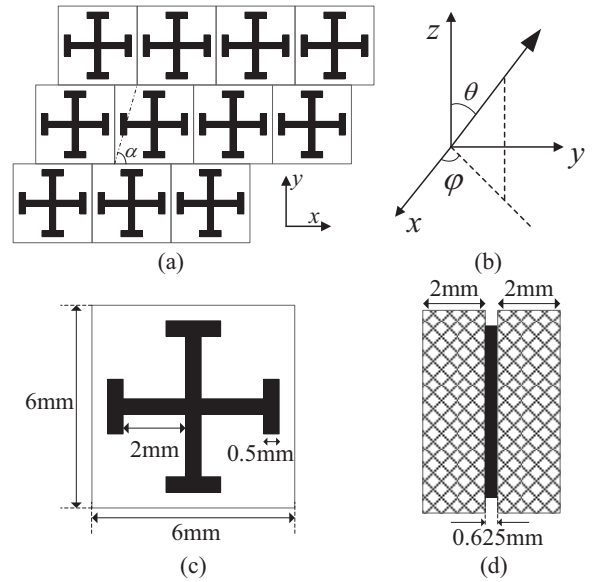


Fig. 3. Schematic diagram of the JCFSS: (a) top view of the skewed periodic JCFSS, (b) direction of the incident plane wave, (c) top view of one unit cell, and (d) side view of one unit cell.

The reflection coefficients of co- and cross-polarizations for both TM and TE cases are presented in Fig. 4. It can be noticed that good agreement between the results of dual plane wave method and results of our wideband method is obtained. However, it can be observed that some sharp peaks of the coefficients might be missed when using the method calculating on individual frequencies, while the wideband method possesses the capacity and advantage to present the details of the frequency response.

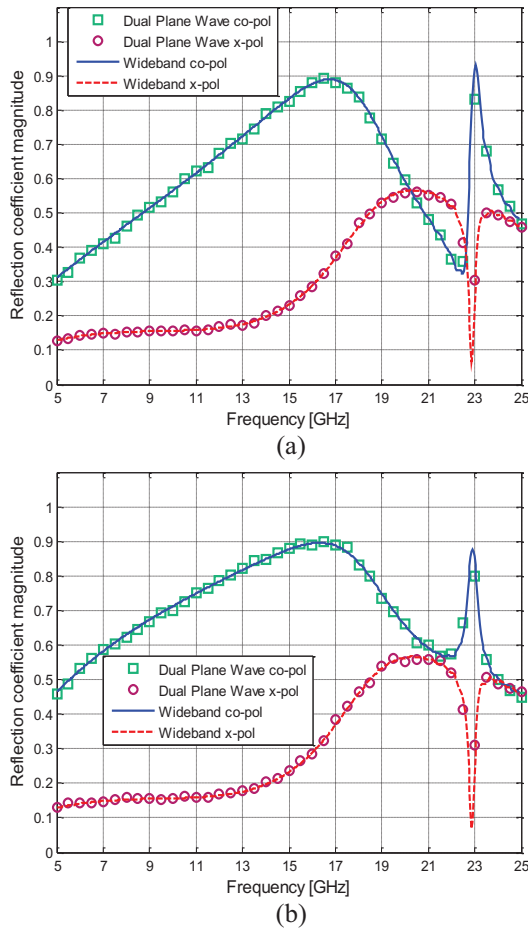


Fig. 4. Reflection coefficient co-polarization and cross polarization for JCFSS oblique incident plane wave ($\theta=30^\circ$, $\varphi=50^\circ$) with skewed angle $\alpha=60^\circ$: (a) TM case and (b) TE case.

IV. CONCLUSION

In conclusion, an efficient FDTD approach for the wideband analysis of arbitrarily skewed periodic structures at oblique incidence is introduced. By proving the field transformation technique to be valid in the skewed PBCs, the split-FDTD is extended to analyze periodic structures with skewed grids. The implementation avoids deliberate calculation of the phase shifts caused by the oblique incidence and the stagger of unit cells. Instead, it presents the PBC as simple as that in the normal incidence. And most significantly, our method realizes the wideband capability to analyze skewed periodic structures at oblique incidence, while the previous related FDTD work require multiple runs in terms of different frequencies. The validity and effectiveness of the method is verified by a numerical example, comparing with the results calculated by the dual plane wave method.

ACKNOWLEDGMENT

This work was supported by National Basic Research Program of China (973 Program) under Grant 2012CB315601.

REFERENCES

- [1] B. A. Munk, *Frequency Selective Surfaces: Theory and Design*, Wiley, 2000.
- [2] T. Wu, *Frequency Selective Surface and Grid Array*, Wiley, 1995.
- [3] R. Mittra, C. H. Chan, and T. Cwik, "Techniques for analyzing frequency selective surfaces - a review," *Proceedings of the IEEE*, vol. 76, no. 12, pp. 1593-1615, 1988.
- [4] Y. Rahmat-Samii and H. Mosallaei, "Electromagnetic band-gap structures: classification, characterization, and applications," in *Editor (Ed.) (Eds.): Book "Electromagnetic band-gap structures: classification, characterization, and applications," IET*, edn., pp. 560-564, 2001.
- [5] N. Amitay, V. Galindo, and C. P. Wu, *Theory and Analysis of Phased Array Antennas*, Wiley, 1972.
- [6] A. Taflov and S. C. Hagness, *Computational Electrodynamics*, Artech House, 2000.
- [7] P. Harms, R. Mittra, and W. Ko, "Implementation of the periodic boundary condition in the finite-difference time-domain algorithm for FSS structures," *Antennas and Propagation, IEEE Transactions on*, vol. 42, no. 9, pp. 1317-1324, 1994.
- [8] J. A. Roden, S. D. Gedney, M. P. Kesler, J. G. Maloney, and P. H. Harms, "Time-domain analysis of periodic structures at oblique incidence: orthogonal and nonorthogonal FDTD implementations," *Microwave Theory and Techniques, IEEE Transactions on*, vol. 46, no. 4, pp. 420-427, 1998.
- [9] J-B.Wang, B. Chen, and B-H. Zhou, "Improved split-field method for solving oblique incident wave on periodic structures," *Electronics Letters*, vol. 47, no. 16, pp. 898-900, 2011.
- [10] Z-Y. Cai, B. Chen, Q. Yin, and R. Xiong, "The WLP-FDTD method for periodic structures with oblique incident wave," *Antennas and Propagation, IEEE Transactions on*, vol. 59, no. 10, pp. 3780-3785, 2011.
- [11] J. Wang, B. Zhou, B. Chen, L. Shi, and C. Gao, "Weakly conditionally stable FDTD method for analysis of 3D periodic structures at oblique incidence," *Electronics Letters*, vol. 48, no. 7, pp. 369-371, 2012.
- [12] B. Liang, M. Bai, H. Ma, N. Ou, and J. Miao, "Wideband analysis of periodic structures at oblique incidence by material independent FDTD algorithm," *Antennas and Propagation, IEEE Transactions on*, vol. 62, no. 1, pp. 354-360,

2014.

[13] Z. Yun and M. F. Iskander, "Implementation of floquet boundary conditions in FDTD analysis of periodic phased array antennas with skewed grid," *Electromagnetics*, vol. 20, no. 5, pp. 445-452, 2000.

[14] K. ElMahgoub, F. Yang, A. Z. Elsherbeni, V. Demir, and J. Chen, "FDTD analysis of periodic structures with arbitrary skewed grid," *Antennas and Propagation, IEEE Transactions on*, vol. 58, no. 8, pp. 2649-2657, 2010.

[15] M. Veysoglu, R. Shin, and J. A. Kong, "A finite-difference time-domain analysis of wave scattering from periodic surfaces: oblique incidence case," *Journal of Electromagnetic Waves and Applications*, vol. 7, no. 12, pp. 1595-1607, 1993.

[16] O. Ramadan, "Auxiliary differential equation formulation: an efficient implementation of the perfectly matched layer," *Microwave and Wireless Components Letters, IEEE*, vol. 13, no. 2, pp. 69-71, 2003.



Ming Bai received the B.Sc. and Ph.D. degrees in Physics, from the University of Science and Technology of China (USTC), in 1996 and 2002, respectively.

From 2002 to 2006, he worked as a Postdoctoral Researcher in the Laboratory of Nanotechnology (LFSP), Spanish National Research Council (CSIC). In

2006, he joined School of Electronic and Information Engineering, Beihang University, as an Associate Professor and was promoted to Professor in 2015. His current research interests include computational electromagnetic and microwave imaging.



Bin Liang received the B.Sc. and Ph.D. degrees in Electronic and Information Engineering from Beihang University, Beijing, China, in 2008 and 2015, respectively.

From 2012 to 2014, he was a Visiting Research Student in School of Engineering and Digital Arts, University of Kent, UK. His research interests include computational electromagnetic, frequency selective surfaces, electromagnetic band-gap structures, and antennas.



Hui Ma received the B.Sc. and Ph.D. degrees in Electronic and Information Engineering from Beihang University, Beijing, China, in 2009 and 2015, respectively.

From 2012 to 2014, she was a Visiting Research Student in Electronic, Electrical and Computer Engineering Department, University of Birmingham, UK. Her research interests include antennas, microwave imaging and passive surface-space bi-static SAR.